This is the accepted manuscript (postprint) of the following article:
Hesar, H. D., & Mohebbi, M. (2020). An adaptive Kalman filter bank for ECG denoising. *IEEE journal of biomedical and health informatics*, *25*(1), 13-21.
https://doi.org/10.1109/JBHI.2020.2982935

An Adaptive Kalman Filter Bank for ECG Denoising

Hamed Danandeh Hesar and Maryam Mohebbi

Abstract— **Model-based Bayesian frameworks proved their effectiveness in the field of ECG processing. However, their performances rely heavily on the pre-defined models extracted from ECG signals. Furthermore, their performances decrease substantially when ECG signals do not comply with their models- a situation generally occurs in the case of arrhythmia-. In this paper, we propose a novel Bayesian framework based on Kalman filter, which does not need a predefined model and can adapt itself to different ECG morphologies. Compared with the previous Bayesian techniques, the proposed method requires much less preprocessing and it only needs to know the location of R-peaks to start ECG processing. Our method uses a filter bank comprised of two adaptive Kalman filters, one for denoising QRS complex (high frequency section) and another one for denoising P and T waves (low frequency section). The parameters of these filters are estimated and iteratively updated using expectation maximization (EM) algorithm. In order to deal with nonstationary noises such as muscle artifact (MA) noise, we used Bryson and Henrikson's technique for the prediction and update steps inside the Kalman filter bank. We evaluated the performance of the proposed method on different ECG databases containing signals having morphological changes and abnormalities such as atrial premature complex (APC), premature ventricular contractions (PVC), Ventricular Tachyarrhythmia (VT) and sudden cardiac death (SCD). The proposed algorithm was compared with several popular ECG denoising methods such as wavelet transform (WD) and empirical mode decomposition (EMD). The comparison results showed that the proposed method performs well in the presence of various ECG morphologies in both stationary and non-stationary environments especially at low input SNRs.**

Index Terms— ECG denoising, Kalman filter, Bayesian filtering, Expectation maximization.

I. Introduction

During the recording of electrocardiogram (ECG) signal, environmental and non-environmental interferences such as noises coming from electrical instruments or electrode misplacement, electromyographic (EMG) noise or muscle artifact (MA), etc. may corrupt its valuable information. Therefore, ECG denoising is considered as an important step in the field of computer-based cardiac analysis and disease diagnosis. Among many techniques proposed for ECG noise reduction, model-based methods are generally favorable because they can preserve morphological and diagnostic features of ECG signal when their models are based on ECG morphology. Among popular model-based techniques, there are Bayesian frameworks such as extended Kalman filters (EKF) [1-3] and marginalized particle extended Kalman filters (MP-EKF) [4, 5]. These approaches use polar variants of a morphological ECG dynamical model (EDM) introduced by McSharry *et al.* [6]. This model describes the ECG beat as a summation of Gaussian kernels corresponding to different ECG feature waves i.e. P, Q, R, S and T. The core structure of these techniques is based on Kalman filter. Although these methods have shown that Kalman filter is handy in different fields of ECG processing such as denoising and segmentation, they have the following problems:

a. They need many preprocessing steps before initialization such as: a) R-peak detection and EDM extraction using an offline nonlinear optimization technique b) Polar phase association to ECG beats c) Kalman filter parameter calculation and estimation of process noise and measurement noise. This problem is universal for every model-based Bayesian framework.
b. They assign a single EDM for an ECG signal. This means that if some ECG beats have significant morphological variations (e.g. in case of arrhythmia, electrode disconnection, etc.), the given EDM is practically useless for those beats. Even though the MP-EKF proposed in [5] can handle such beats using its adaptive fuzzy-based particle weighting strategy, it cannot perform well when there is no proper EDM for an ECG signal. This situation happens when the number of normal beats are less than abnormal beats.
c. The process and measurement noise matrices for Kalman

H. Danandeh Hesar is with the Faculty of Biomedical Engineering, Sahand University of Technology, Tabriz, Iran and the Department of Biomedical Engineering K. N. Toosi University of Technology, Tehran, Iran and (e-mails: danandeh@sut.ac.ir, h_danandeh@ee.kntu.ac.ir).
M. Mohebbi is with the Department of Biomedical Engineering, K. N. Toosi University of Technology, Tehran, Iran (e-mail: m.mohebbi@kntu.ac.ir).

This is the accepted manuscript (postprint) of the following article:
Hesar, H. D., & Mohebbi, M. (2020). An adaptive Kalman filter bank for ECG denoising. *IEEE journal of biomedical and health informatics*, *25*(1), 13-21.
https://doi.org/10.1109/JBHI.2020.2982935

filter are not updated through the filtering procedure. This means that if these matrices are not properly defined before filtering procedure or the properties of noises change from one beat to another beat, the outputs of these filters are not trustworthy.

In order to overcome the above problems, in this paper, we propose a novel Bayesian framework, which employs a Kalman filter bank and expectation maximization (EM) algorithm for ECG processing. The contributions of this paper is as follows:

1- This method needs only an R-peak detection step before initialization. Using the locations of R-peaks, we can separate each ECG beat into two sections: QRS complex (high frequency section) and P-T waves (low frequency section). The QRS segments from ECG beats are appended together to form a high-frequency signal. P-T waves appended together as well to construct a low-frequency signal. These two signals are fed into the proposed Kalman filter bank.
2- The Kalman filter bank in this method is comprised of two independent Kalman filters that denoise the aforementioned high and low-frequency signals.
3- The parameters of two Kalman filters are estimated and iteratively updated using EM algorithm.
4- In order to handle non-stationary noises, we exploit the Bryson and Henrikson's technique [7] for the prediction and update steps inside the Kalman filter bank.

This paper is organized as follows: Section II briefly explains the theory of Kalman filter and estimation of its parameters using EM algorithm. In the last part of section II the Bryson and Henrikson's method is described. Section III focusses on the proposed denoising method. The experimental results and analyses are given in Section IV and finally conclusions are drawn in the last section.

II. Mathematical Preliminaries

In this section, the equations of Kalman filter and EM algorithm are reviewed. In addition, the modifications suggested for handling colored measurement noise in Kalman filter are explained.

A. Kalman Filter

Kalman filter is an efficient Bayesian recursive linear quadratic estimation (LQE) technique that can estimate the unknown variables from series of noisy and inaccurate measurements observed over time. It can be shown that the recursive sequential estimation procedure in Kalman filter is more precise than other methods based on a single measurement alone [8]. The Kalman filter algorithm is simple and straightforward. Its variants were successfully implemented in a wide range of applications such as signal denoising, robotics, guidance, navigation, and control of vehicles, particularly aircraft and spacecraft.

The general state-space and measurement models in discrete-time Kalman filter are as following:

$$\mathbf{x}_k = A_k\mathbf{x}_{k-1} + \mathbf{w}_{k-1} \quad (1.a)$$
$$\mathbf{y}_k = C_k\mathbf{x}_k + \mathbf{v}_k \quad (1.b)$$

where $\mathbf{x}_k, y_k, A_k, C_k$ are state vector, measurement vector, transition matrix and measurement matrix at time step k respectively. In that order, $\mathbf{v}_k$ and $\mathbf{w}_k$ are measurement and process noise vectors at the time step k. These two noise vectors, model the uncertainties of measurement and state dynamics using normal "white" Gaussian noise with corresponding covariance matrices R_k ($\mathbf{v}_k \sim \mathcal{N}(0, R_k)$) and Q_k ($\mathbf{w}_k \sim \mathcal{N}(0, Q_k)$).

Using (1), the discrete Kalman filter algorithm can be summarized in the following two stages namely "prediction" and "update" steps:

a. Prediction step:

$$\hat{\mathbf{x}}_{k|k-1} = A_k\hat{\mathbf{x}}_{k-1|k-1} \quad (2.a)$$
$$P_{k|k-1} = A_kP_{k-1|k-1}A_k^T + Q_{k-1} \quad (2.b)$$

b. Update step:

$$\mathbf{i}_k = \mathbf{y}_k - C_k\hat{\mathbf{x}}_{k|k-1} \quad (3.a)$$
$$S_k = C_kP_{k|k-1}C_k^T + R_k \quad (3.b)$$
$$K_k = P_{k|k-1}C_k^TS_k^{-1} \quad (3.c)$$
$$\hat{\mathbf{x}}_{k|k} = \hat{\mathbf{x}}_{k|k-1} + K_k\mathbf{i}_k \quad (3.d)$$
$$P_{k|k} = P_{k|k-1} - K_kS_kK_k^T \quad (3.e)$$

where $\hat{\mathbf{x}}_{k|k-1}$ and $\hat{\mathbf{x}}_{k|k}$ are predicted and updated (estimated) means of state vector at time step k respectively. In that order, $P_{k|k-1}$ and $P_{k|k}$are predicted and updated covariance matrices of state vector at time step k. $\mathbf{i}_k, K_k$ and S_k are innovation vector, Kalman filter gain and measurement prediction error covariance matrix accordingly. Kalman filter is initialized with the prior (initial) distribution for the state vector $\mathbf{x}_0 \sim N(\mathbf{m}_0, P_0)$. Parameters $\mathbf{m}_0$and P_0 are chosen based on prior information about the system under the study.

The marginal likelihood of Kalman filter is defined as following:

$$p(Y_N) = \prod_{k=0}^{N} p(\mathbf{y}_k|\mathbf{y}_{k-1}, \dots, \mathbf{y}_0) \quad (4)$$

where $Y_N = \{\mathbf{y}_1, \mathbf{y}_2, \dots, \mathbf{y}_k, \dots, \mathbf{y}_N\}$. Using the update step in (3), the *log* marginal likelihood of Kalman filter can be recursively calculated as [9]:

$$\ell_k = \ell_{k-1} - \frac{1}{2}(\mathbf{i}_k^TS_k^{-1}\mathbf{i}_k + \log|S_k| + N_{\mathbf{y}}\log 2\pi) \quad (5)$$

where $N_{\mathbf{y}}$ is the dimension of measurement vector $\mathbf{y}_k$.

The outputs of Kalman filter can be further smoothed using backward-pass methods such as Rauch–Tung–Striebel (RTS) smoother [10]. This method is summarized in the following equations:

$$L_k = P_{k|k}A_{k+1}^TP_{k+1|k}^{-1} \quad (6.a)$$
$$\hat{\mathbf{x}}_{k|N} = \hat{\mathbf{x}}_{k|k} + L_k(\hat{\mathbf{x}}_{k+1|N} - \hat{\mathbf{x}}_{k+1|k}) \quad (6.b)$$
$$P_{k|N} = P_{k|k} + L_k(P_{k+1|n} - P_{k+1|k})L_k^T \quad (6.c)$$

where $\hat{\mathbf{x}}_{k|N}$ and $P_{k|N}$ are the smoothed state estimate and covariance matrix generated in the backward pass at time step k respectively.

This is the accepted manuscript (postprint) of the following article:
Hesar, H. D., & Mohebbi, M. (2020). An adaptive Kalman filter bank for ECG denoising. *IEEE journal of biomedical and health informatics*, *25*(1), 13-21.
https://doi.org/10.1109/JBHI.2020.2982935

B. Expectation Maximization Algorithm for Kalman Filter

Despite its efficiency and simplicity, the Kalman filter suffers from one major problem. In order to estimate the unknown variables properly, the building parameters of eqns. (2) and (3) i.e. $\{A_k, C_k, Q_k, R_k, \mathbf{m}_0, P_0\}$ should be identified correctly (especially Q_k and R_k). EM algorithm can exploit the outputs of Kalman smoother to identify the system dynamics [9, 11, 12].

It is known that for a particular set of probabilistic measurements $Y_N = \{\mathbf{y}_1, \dots \mathbf{y}_k, \dots, \mathbf{y}_N\}$, the maximum likelihood (ML) estimate of probabilistic parameter set $\boldsymbol{\theta}$ is acquired by maximizing the marginal likelihood of $\mathbf{y}_{1:N}$ with respect to $\boldsymbol{\theta}$, that is to say**:**

$$\widehat{\boldsymbol{\theta}}_{ML} = \underset{\boldsymbol{\theta}}{\operatorname{argmax}}(log\ p_{\boldsymbol{\theta}}(\mathbf{y}_{1:N})) \tag{7}$$

In case of unknown linear Gaussian state-space system defined in (1), the probabilistic parameter set that we desire to identify is $\boldsymbol{\theta} = \{A_k, C_k, Q_k, R_k, \mathbf{m}_0, P_0\}$. For simplicity, let's suppose that A_k, C_k, Q_k and R_k are constant for all time steps i.e. $\boldsymbol{\theta} = \{A, C, Q, R, \mathbf{m}_0, P_0\}$. Using EM method and the *log* marginal likelihood of Kalman filter, the ML estimate of $\boldsymbol{\theta}$ **is** obtained using the outputs of RTS smoother in the following two steps:

1- The *E*-step: it involves computing the expectation of *log* likelihood $\mathcal{O}(\boldsymbol{\theta}, \boldsymbol{\theta}_i) = E[\log p_{\boldsymbol{\theta}_i}(\mathbf{y}_{1:N}, \mathbf{x}_{1:N} | \mathbf{y}_{1:N})]$ given the estimated parameters of $\boldsymbol{\theta}$ at *i*th iteration. The quantity of $\mathcal{O}$ is determined by the following [9, 13]:

$$E[\mathbf{x}_k|\mathbf{y}_{1:N}] = \hat{\mathbf{x}}_{k|N} \tag{8.a}$$

$$S_{1,1,k} = E[\mathbf{x}_k\mathbf{x}_k^T|\mathbf{y}_{1:N}] = P_{k|N} + \hat{\mathbf{x}}_{k|N}\hat{\mathbf{x}}_{k|N}^T \tag{8.b}$$

$$S_{1,0,k} = E[\mathbf{x}_k\mathbf{x}_{k-1}^T|\mathbf{y}_{1:N}] = P_{k,k-1|N} + \hat{\mathbf{x}}_{k|N}\hat{\mathbf{x}}_{k-1|N}^T \tag{8.c}$$

$$S_{0,0,k} = E[\mathbf{x}_{k-1}\mathbf{x}_{k-1}^T|\mathbf{y}_{1:N}] = P_{k-1|N} + \hat{\mathbf{x}}_{k-1|N}\hat{\mathbf{x}}_{k-1|N}^T \tag{8.d}$$

where

$$P_{k,k-1|N} = P_{k|k}L_{k-1}^T + L_k\,(P_{k+1,k|N} - P_{k|k})L_{k-1}^T \tag{9}$$

which is initialized by $P_{N,N-1|N} = (I - K_N)P_{N-1|N-1}$ [9, 13].

2- The *M*-step: it involves re-estimation of model parameters by maximizing the $\mathcal{O}$ over $\boldsymbol{\theta}$ using partial derivatives of $\mathcal{O}$ and setting them to zero. Solving these equations yields the updated parameters (in the *i*th iteration) as following:

$$A^{(i)} = (\textstyle\sum_{k=2}^N S_{1,0,k})(\sum_{k=2}^N S_{0,0,k})^{-1} \tag{10.a}$$

$$Q^{(i)} = \frac{1}{N-1}(\textstyle\sum_{k=2}^N S_{1,1,k} - A^{(i)}(\sum_{k=2}^N S_{1,0,k})^{\boldsymbol{T}}) \tag{10.b}$$

$$C^{(i)} = (\sum_{k=1}^{N} \mathbf{y}_k\hat{\mathbf{x}}_{k|N}^T)(\sum_{k=1}^{N} P_{k|N})^{-\mathbf{1}} \tag{10.c}$$

$$R^{(i)} = \frac{1}{N}(\textstyle\sum_{k=1}^N(\mathbf{y}_k - C^{(i)}\hat{\mathbf{x}}_{k|N})(\mathbf{y}_k - C^{(i)}\hat{\mathbf{x}}_{k|N})^{\boldsymbol{T}} - C^{(i)}P_{k|N}(C^{(i)})^{\boldsymbol{T}}) \tag{10.d}$$

$$P_0^{(i)} = P_{1|N} \tag{10.e}$$

$$\mathbf{m}_0^{(i)} = \hat{\mathbf{x}}_{1|N} \tag{10.f}$$

The above equations offer a formal form for EM algorithm. However, EM can be implemented in a more numerically robust and efficient approach detailed in [11].

C. Handling Colored Measurement Noise

If the building parameters of Kalman filter are correctly chosen, it can optimally estimate the unknown variables in the white Gaussian stationary environment. However, if the process or the measurement noises or both of them are colored, the Kalman filter outputs are not optimal. An example of a colored noisy environment is the following system:

$$\mathbf{x}_k = A_k\mathbf{x}_{k-1} + \mathbf{w}_{k-1} \tag{11.a}$$

$$\mathbf{y}_k = C_k\mathbf{x}_k + \mathbf{v}_k \tag{11.b}$$

$$\mathbf{v}_k = \psi_k\mathbf{v}_{k-1} + \mathbf{e}_k \tag{11.c}$$

where ψ_k is measurement noise transition matrix and $\mathbf{e}_k$ is white Gaussian noise with covariance matrix R_k ($\mathbf{e}_k \sim \mathcal{N}(0, R_k)$). The values of elements in ψ_k describe the type of noise present in measurements. Small values in ψ_k indicate that the measurement noise is closely similar to stationary white Gaussian noise. High values in ψ_k indicate that the measurement noise has strong nonstationary features. Although the system in (11) is defined generally for non-stationary environments, we can implement Kalman filter for such system using a trick called the "measurement time-difference" approach [7, 12, 14]. In this procedure, the following pseudo-measurement is defined in order to whiten the colored measurement noise:

$$\mathbf{z}_k = \mathbf{y}_{k+1} - \psi_k\mathbf{y}_k \tag{12}$$

Using the above equation, the parameters in eqns. (2) and (3) are modified in the following way [7, 12]:

$$C_{k,new} = C_kA_k - \psi_kC_k \tag{13.a}$$

$$S_k = Q_kC_k^T \tag{13.b}$$

$$R_{k,new} = C_kQ_kC_k^T + R_k \tag{13.c}$$

$$J_k = S_kR_{k,new}^{-1} \tag{13.d}$$

$$Q_{k,new} = Q_k + S_kR_{k,new}^{-1}S_k^T \tag{13.e}$$

$$A_{k,new} = A_k - J_kC_{k,new} \tag{13.f}$$

where $A_{k,new}, C_{k,new}, Q_{k,new}$ and $R_{k,new}$ are the modified building parameters of the Kalman filter for system in (11). Based on the above equations, the prediction and update steps of Kalman filter designed for system in (11) are as following [7, 12]:

a. Prediction step:

$$\hat{\mathbf{x}}_{k|k-1} = A_{k,new}\hat{\mathbf{x}}_{k-1|k-1} + J_k(\mathbf{z}_{k-1} - C_{k,new}\hat{\mathbf{x}}_{k-1|k-2}) \tag{14.a}$$

$$P_{k|k-1} = A_{k,new}P_{k-1|k-1}A_{k,new}^T + Q_{k-1,new} \tag{14.b}$$

b. Update step:

$$\mathbf{i}_k = \mathbf{z}_k - C_{k,new}\hat{\mathbf{x}}_{k|k-1} \tag{15.a}$$

$$S_k = C_{k,new}P_{k|k-1}C_{k,new}^T + R_{k,new} \tag{15.b}$$

$$K_k = P_{k|k-1}C_{k,new}^TS_k^{-1} \tag{15.c}$$

$$\hat{\mathbf{x}}_{k|k} = \hat{\mathbf{x}}_{k|k-1} + K_k\mathbf{i}_k \tag{15.d}$$

$$P_{k|k} = P_{k|k-1} - K_kS_kK_k^T \tag{15.e}$$

III. Proposed Method for ECG Denoising

In this section, we explain our method for ECG denoising. It is known that an ECG beat contains both high frequency and low frequency segments, which means it has nonlinear dynamics. Therefore, a good denoising performance cannot be

This is the accepted manuscript (postprint) of the following article:
Hesar, H. D., & Mohebbi, M. (2020). An adaptive Kalman filter bank for ECG denoising. *IEEE journal of biomedical and health informatics*, *25*(1), 13-21.
https://doi.org/10.1109/JBHI.2020.2982935

accomplished with a single Kalman filter. In this paper, we employed two separate Kalman filters as a filter bank to deal with this nonlinearity. One Kalman filter is designed to handle QRS complexes (high frequency parts), the other one is dedicated to P and T segments (low frequency parts). The parameters of each Kalman filter are independently and adaptively approximated using the EM algorithm explained in section II.B. Our algorithm initializes with R-peak detection. The R peaks of input ECG signal are extracted using the well-known Pan-Tompkins method. Contrary to other model-based methods, which require several heavy preprocessing steps, R-peak detection is the only preprocessing step needed for our algorithm. Regarding this fact that the duration of a QRS complex in normal ECG beat is not more than 0.12 seconds [15], the samples belonging to QRS complexes are extracted from ECG signal using time windows around the locations of R-peaks. Since the durations of RS waves are often longer than QR waves, the time windows are placed unevenly around R-peaks. We assume that 40% of each time window belongs to QR (0.048 seconds) wave and 60% to RS wave (0.072 seconds). The samples belonging to these time windows are regarded as QRS waves. The remaining samples are assumed to be belonging to either P or T waves (or U waves). For better understanding, the next step is depicted in Fig.1 for a segment from record ‘16272’ from MIT-BIH Normal Sinus Rhythm database (NSRDB)[16]. In this step, QRS complexes from successive beats are concatenated together to build a high frequency signal (see Fig.1 (b)). P and T waves are also chained together from consecutive beats to form a low frequency signal (see Fig.1(c)). After that, these two signals are fed into a Kalman filter bank. In this filter bank, there are two independent Kalman filters. One Kalman filter is dedicated to process QRS waves and the other is designed to process P & T waves. Using EM algorithm and RTS smoother equations, the filter bank denoise the aforementioned signals using the iterative process of the EM algorithm. It is worth to mention that for each Kalman filter, an independent EM algorithm is used. In the final step, the two denoised signals are reassembled to construct the denoised ECG signal. It is worth reminding that unlike the convolution-based filters, the size of input is equal to the size of output in Kalman filter frameworks. Therefore, the problem of mismatching samples in the reassembling process is avoided in the proposed algorithm. In order to manage the nonstationary noises more effectively, we propose to use the modified model defined in equations (11-15) instead of standard model defined in equations (1-3). Moreover, in nonstationary noises, our algorithm has one more post processing step to suppress baseline drifts. In this step, we use a median filter to remove baseline drifts.

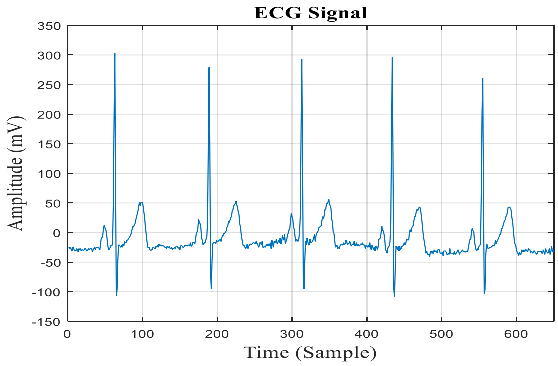

(a)

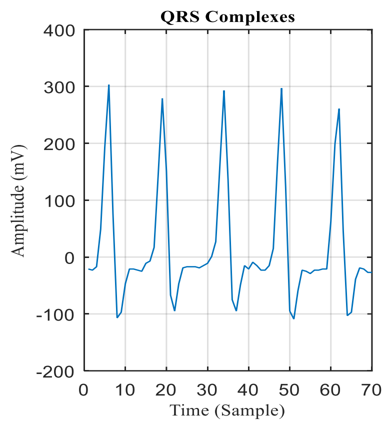

(b)

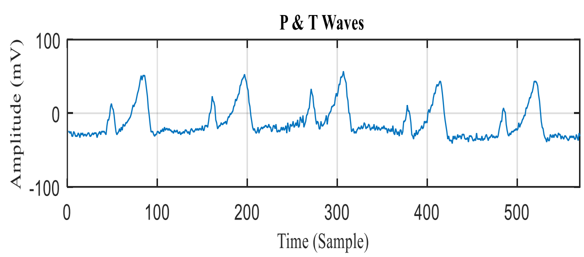

(c)

Fig. 1- The proposed procedure for extraction of low and high frequency parts of an ECG signal. (a) ECG segment from record ‘16272’ (b) Concatenated high frequency QRS complexes (c) Concatenated low frequency P and T waves.

Fig. 2 illustrates the flowchart of the proposed method. From Fig. 2, it is realized that our algorithm only needs to know the locations of R peaks in ECG signal. It does not need any information about ECG dynamics contrary to other Bayesian methods such as EKF and MP-EKF. In addition, in the aforementioned EKF and MP-EKF based methods, we are restricted to work with ECG segments having normal beats or beats that comply with the predefined EDMs. However, our algorithm can be even used in ECG segments having several dynamics. This feature enables us to process ECG signals having various kinds of arrhythmias or having lead disconnection. Moreover, our algorithm can be implemented in extreme situations such as ventricular tachyarrhythmia (VT) or sudden cardiac death (SD) in which ECG signals lose most of their feature characteristics and exhibit very different dynamics.

This is the accepted manuscript (postprint) of the following article:
Hesar, H. D., & Mohebbi, M. (2020). An adaptive Kalman filter bank for ECG denoising. *IEEE journal of biomedical and health informatics*, *25*(1), 13-21.
https://doi.org/10.1109/JBHI.2020.2982935

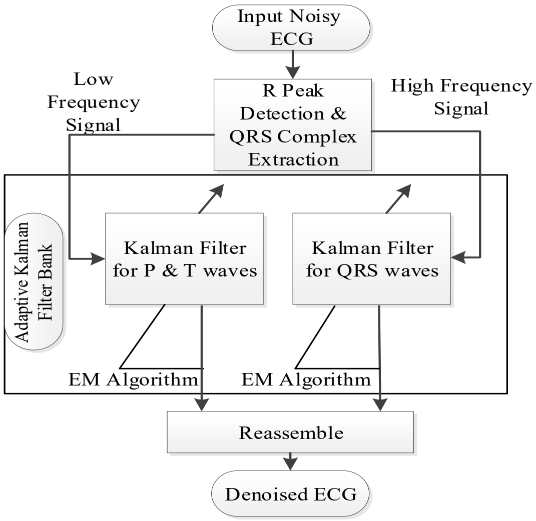

Fig. 2- Flowchart of the proposed denoising algorithm.

In the next section, we provide some illustrative examples about how our algorithm works in different conditions mentioned above. Moreover, the dynamic models in our algorithm are updated through filtering process where in previous Bayesian methods; the dynamic models are unchanged during the filtering process.

IV. The Experimental Results

The performance of the proposed algorithm was investigated on several ECG segments extracted from four online PhysioBank databases. The databases were MIT-BIH normal sinus rhythm (NSRDB) [16], MIT-BIH arrhythmia (ADB) [17], Creighton university ventricular tachyarrhythmia (CUDB) [18] and sudden cardiac death Holter databases (SCDB) [19]. The ECG signals in the aforementioned databases were recorded at sampling rates of 128, 360, 250 and 250 Hz respectively. Two hundred (200) ECG segments from different records of NSRDB were selected which contained only normal beats. This database was selected in order to evaluate the performance of the proposed filter bank in normal ECG segments with no distinguishable dynamic changes. The duration of each segment was 30 seconds. Forty-four (44) ECG segments from various records of ADB were chosen in order to investigate the performance of the proposed method in case of sudden changes in dynamics such as arrhythmia. Each segment from this database contained arrhythmic beats. These abnormal beats were related to either premature ventricular contraction (PVC) or atrial premature complex (APC). The duration of each segment from this database was 1-2 minutes. The average duration of arrhythmic beats in each segment was almost 9 seconds (15% of total duration). In order to evaluate the performance of our algorithm in situations where there are considerable changes in ECG dynamics and morphology, we selected 20 segments from 20 records of SCDB and 30 segments from 30 records of CUDB. The durations of these segments varied between one to three minutes. The percentage of arrhythmic beats in the segments from CUDB and SCDB was over 30%.

For initialization, the dimensions of building parameters inside the adaptive Kalman filters should be well defined. Since we had single lead noisy ECG signals as measurements, the matrices C, R (and ψ) were 1×1 matrices for both Kalman filters consequently. The transition matrix A was considered as a 3×3 upper triangular matrix giving more flexibility to performance of Kalman filters. Larger dimensions were also tested for transition matrices, but because we chose single-lead ECG measurements, the corresponding filtering results showed insignificant improvement.

Using the above configuration for building parameters of Kalman filters, the denoising performance of proposed method was investigated in two types of noises: artificial white Gaussian noise and real muscle artifact noise. The real muscle artifacts are extracted from the MIT-BIH Noise Stress Test Database [20]. These noises were recorded at a sampling rate of 360 Hz and needed to be resampled with respect to sampling frequencies of evaluation databases. Twelve different input SNRs ranging from 10 to -5dB were considered for evaluation. For illustrative purpose, the denoising performance of the adaptive Kalman filter bank in the presence of white Gaussian noise in several databases is shown in Fig. 3. In this figure, the original clean ECGs are plotted in elevated positions for better visualization. As you can see in Figs. 3 (a) and (b), our algorithm performs well in both normal beats and arrhythmic ones. In Fig. 3(b), there are four PVC beats along with several normal beats at the end. The morphologies of PVC beats are considerably different from the morphologies of normal beats. However, our algorithm managed to suppress the noise and adapt its building parameters to keep track of both normal and abnormal beats. Figs. 3(c) and (d) show two examples of situations where there are several drastic changes in ECG dynamics and morphology in consecutive beats. It can be seen in these two figures that the proposed algorithm exhibited acceptable results in these kinds of situations.

For quantitative assessment, the SNR improvement metric and for qualitative assessment the “Multi-Scale Entropy Based Weighted Distortion Measure” (MSEWPRD) [21] were calculated for each segment at each input SNR. The SNR improvement metric is given by:

$$\mathrm{imp}[\mathrm{dB}] = \mathrm{SNR}_{\mathrm{output}} - \mathrm{SNR}_{\mathrm{input}} = 10\log\left(\frac{\sum_i \left|x_n(i) - x_o(i)\right|^2}{\sum_i \left|x_d(i) - x_o(i)\right|^2}\right) \quad (15)$$

where x_o, x_n and x_d denote the original ECG signal, the noisy ECG signal and the denoised ECG signal, respectively [2]. In

This is the accepted manuscript (postprint) of the following article:
Hesar, H. D., & Mohebbi, M. (2020). An adaptive Kalman filter bank for ECG denoising. *IEEE journal of biomedical and health informatics*, *25*(1), 13-21.
https://doi.org/10.1109/JBHI.2020.2982935

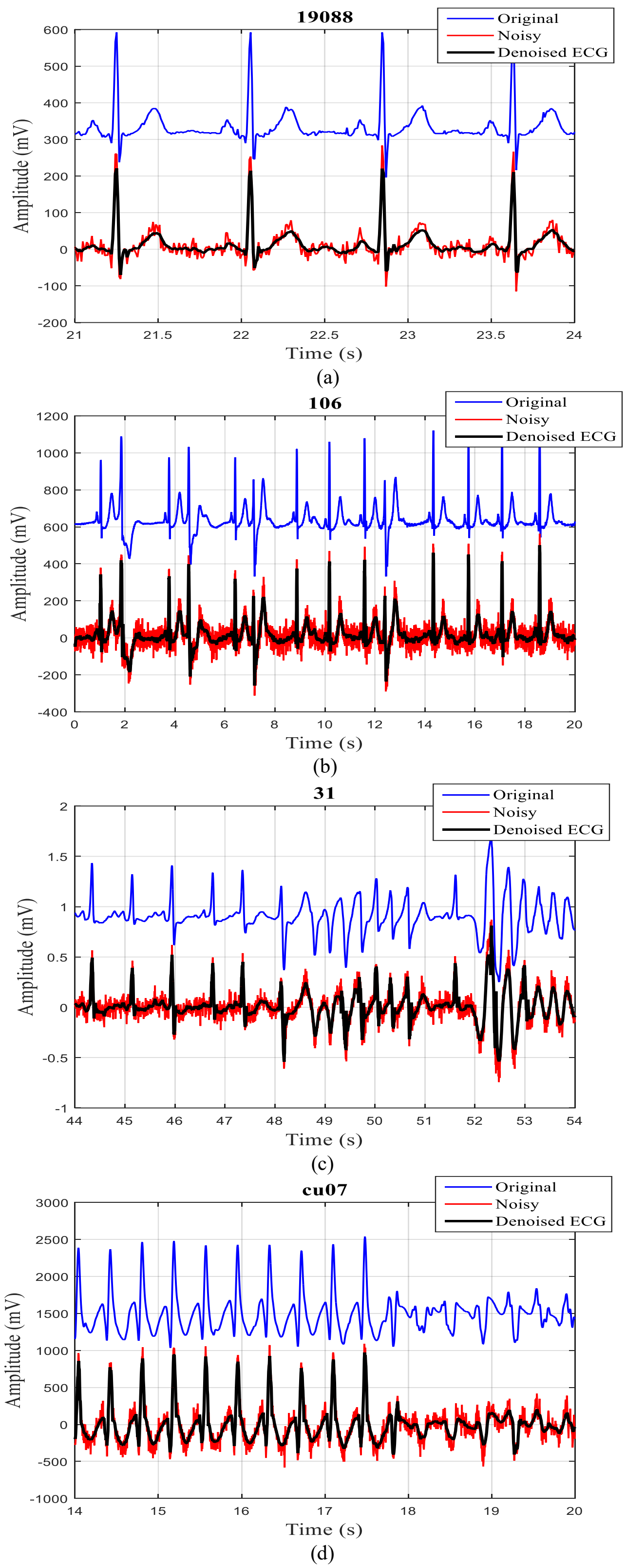

Fig. 3- Performance of the proposed adaptive filter bank in the presence of white Gaussian noise for records a) 19088 from NSRDB at SNR =6dB b) 106 from ADB at SNR = 4dB c) 31 from SCDB at SNR= 4dB d) cu07 from CUDB at SNR = 8 dB

order to calculate the MSEWPRD metric, both original are calculated in different sub bands and weighted percentage root-mean-square differences (WPRD) between these entropies are computed and regarded as MSEWPRD [21]. This qualitative metric represents how well a denoising algorithm preserves the diagnostic features of original ECG signal. The benchmark methods in this paper comprised of popular non-model-based methods such as ensemble empirical mode decomposition (EEMD) [22], band pass filter (BPF) and wavelet-based denoising scheme [23]. The FIR band pass filter in this paper had a pass band range of 0.4-25 Hz. For denoising using wavelet, the Daubechies-4 (DB4) mother wavelet was chosen. The shrinkage rule was the Heuristic *Stein's Unbiased Risk Estimate* (Heuristic SURE) along with multi-level rescaling and soft thresholding strategy.

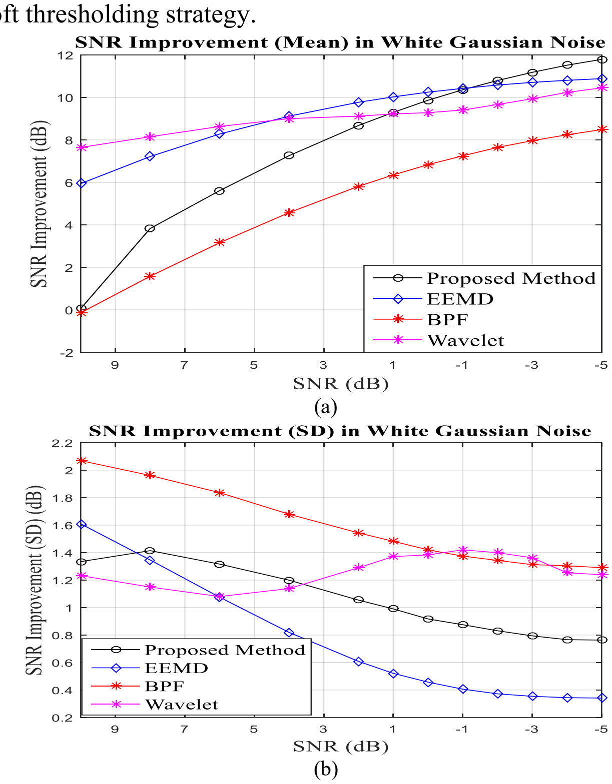

Fig. 4-Performance evaluation of the denoising methods in all 4 databases from (a) SNR improvement mean and (b) SNR improvement SD viewpoints.

Figures 4 and 5 represent the overall denoising performance of the proposed Kalman filter bank, EEMD, BPF and wavelet frameworks for all four databases in the presence of white Gaussian noise from SNR improvement and MSEWPRD viewpoints. By looking at these two figures, it can be realized that the proposed method outperformed BPF at all input SNRs. It is also evident that the wavelet-based framework has the best performance for high input SNRs and EEMD framework performed best at mid-range input SNRs. As input SNR decreases from 1 dB to -5dBin this figure, the performance of our denoising framework exhibits the best results from SNR improvement viewpoint. Moreover, it can be seen that both EEMD and the adaptive Kalman filter bank outperformed other methods in very noisy environments from MSEWPRD

This is the accepted manuscript (postprint) of the following article:
Hesar, H. D., & Mohebbi, M. (2020). An adaptive Kalman filter bank for ECG denoising. *IEEE journal of biomedical and health informatics*, *25*(1), 13-21.
https://doi.org/10.1109/JBHI.2020.2982935

viewpoint. Overall, it can be inferred that in very noisy situations, the adaptive Kalman filter bank is a suitable choice for white Gaussian noise reduction. Figures 4 and 5 show that the proposed adaptive framework can be implemented in very noisy environments and used for decontamination of many kinds of ECG signals without having concerns about models or the morphologies of ECG signals.

Table I. Performance evaluation of the proposed method filtering frameworks for all four databases in the presence of MA noise from SNR improvement viewpoint.

	SNR IMPROVEMENT $(mean \pm SD)$ (DB) **in MA noise**					
ψ	10 DB	6 DB	2 DB	0 DB	-2 DB	-5 DB
0.01	0.783± 1.901	3.858± 1.646	6.274± 1.325	7.195± 1.173	7.93± 1.05	8.734± 0.941
0.1	0.561± 1.943	3.711± 1.699	6.233± 1.381	7.214± 1.223	8.005± 1.091	8.88± 0.967
0.2	0.276±2 .024	3.524± 1.771	6.202± 1.413	7.272± 1.221	8.159± 1.049	9.165± 0.891
0.3	-0.063± 2.079	3.266± 1.851	6.073± 1.512	7.23± 1.303	8.195± 1.113	9.308± 0.912
0.4	-0.913± 1.908	2.628± 1.768	5.79± 1.54	7.158± 1.374	8.355± 1.21	9.79± 0.991
0.5	-0.932± 2.266	2.588± 2.062	5.692± 1.739	7.016± 1.53	8.156± 1.322	9.534± 1.02
0.6	-0.945± 2.276	2.588± 2.062	5.692± 1.739	7.016± 1.53	8.156± 1.322	9.544± 1.02

In order to investigate the advantage of using the Bryson & Henrikson's model in (11) over the standard model in (1) inside the proposed adaptive framework, the denoising performance of adaptive Kalman filter bank was evaluated in the presence of muscle artifact noise for different values of ψ. As shown in Table I, the lowest value of ψ was 0.01. With this value, the modified model in (11) is very similar to standard model in (1). In other words, the results obtained by choosing $\psi = 0.01$ represent the case in which the adaptive Kalman filter bank did used its standard model for denoising non-stationary MA noise. It can be seen in Table I that as ψ increases to values near 0.4, the performance of the adaptive Kalman filter bank improves from both SNR improvement and MSEWPRD viewpoints. For values greater than 0.4, the denoising performance of the proposed filter bank declines at mid-range SNRs. The results in Table I implies two facts: 1- Using the proposed modified model in (11), improves the performance of adaptive Kalman filter bank significantly in handling non-stationary noises. 2- The appropriate value for ψ for denoising MA noise is approximately 0.4. In Figures 6 and 7, we compared the denoising performance of the proposed adaptive Kalman filter bank (for $\psi = 0.4$) with EEMD, BPF and wavelet for records

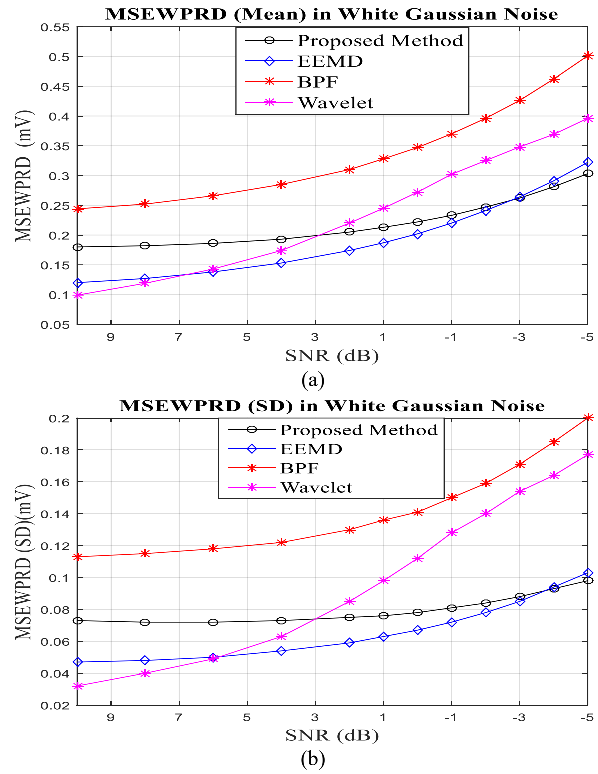

Fig. 5-Performance evaluation of the denoising methods in all 4 databases from (a) MSEWPRD mean and (b) MSEWPRD SD viewpoints.

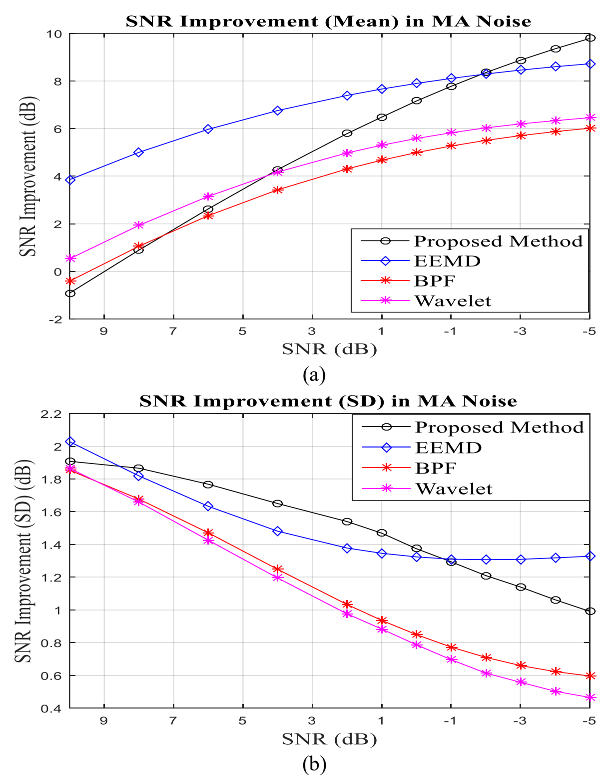

Fig. 6-Performance evaluation of the denoising methods in all 4 databases from (a) SNR improvement mean and (b) SNR improvement SD viewpoints.

of all four databases in the presence of MA noise from SNR

This is the accepted manuscript (postprint) of the following article:
Hesar, H. D., & Mohebbi, M. (2020). An adaptive Kalman filter bank for ECG denoising. *IEEE journal of biomedical and health informatics*, *25*(1), 13-21.
https://doi.org/10.1109/JBHI.2020.2982935

improvement and MSEWPRD viewpoints. It can be seen from these two figures that the proposed framework outperformed the non-model based methods in nonstationary environments at low input SNRs thanks to its modified model and adaptive strategy.

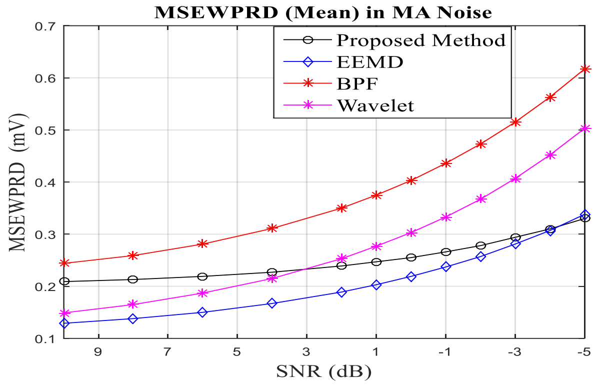

(a)

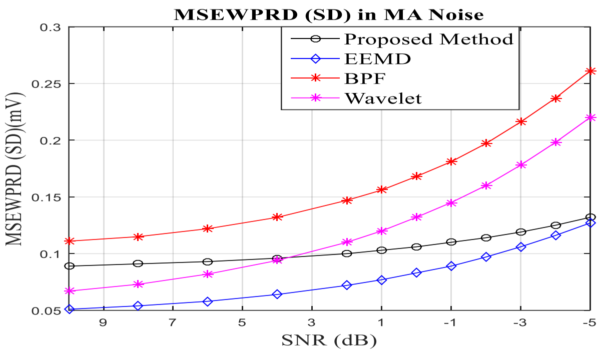

(b)

Fig. 7-Performance evaluation of the denoising methods in all 4 databases from (a) MSEWPRD mean and (b) MSEWPRD SD viewpoints.

It is important to know that, in order to draw a much fairer comparison between our proposed method and benchmark methods, the denoising results should be separately evaluated for all of the records of each database. We accomplished this task and separated the comparison results for each database. However, due to page number limitation, the results are reported in a supplementary document that is available for readers. The separated evaluation results indicated that the proposed adaptive Kalman filter bank performed well in all four databases specifically at nonstationary environments and at low inputs SNRs. We also included model-based Bayesian methods such as MP-EKF, EKF and EKS in benchmark evaluation of this paper and added them into the supplementary document. But, as said earlier, these methods cannot be used in ECG records that have various kinds of ECG dynamics. Moreover, they cannot be used in ECG signals in which it is impossible to extract a proper EDM. Therefore, we are unable to evaluate EKF/EKS and MP-EKF frameworks for records of SCDB and CUDB. However, MP-EKF can handle slight changes in morphology of signal using its adaptive particle weighting strategy. Therefore, it can be evaluated on records from ADB.

V. Discussion

The Kalman filter bank presented in this paper does not need a predefined model and can adapt itself to different ECG dynamics and morphologies in stationary/nonstationary environments. An example of filtering in the presence of nonstationary MA noise is demonstrated in Fig. 8. In this figure, several kinds of ECG beats with different kinds of morphologies are present. Similar to Fig. 3, for better realization, the original clean ECGs are plotted in elevated positions in this figure. In Fig. 8(a), before adding the MA noise, the original ECG is itself contaminated with an unknown kind of noise. Moreover, a PVC beat can be observed in this figure which has a significant morphological difference with other beats. However, the adaptive filter bank managed to suppress the noise sufficiently well while keeping the morphological properties of all ECG beats. In Fig. 8(b), a situation is presented where there are different kinds of normal and abnormal beats contaminated with nonstationary MA noise. The proposed Kalman filter banks once again managed to deal with this case successfully thanks to its adaptive EM algorithm and its modified model.

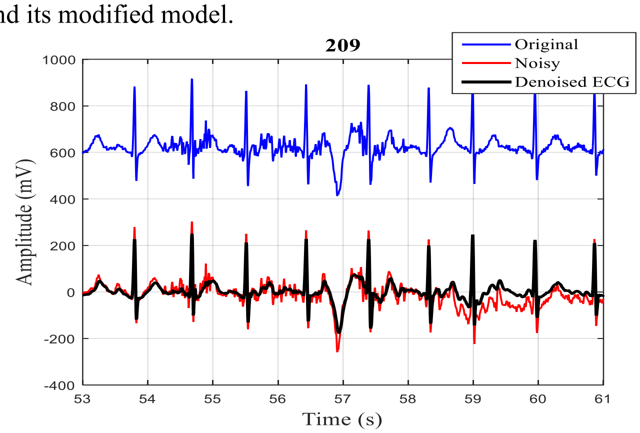

(a)

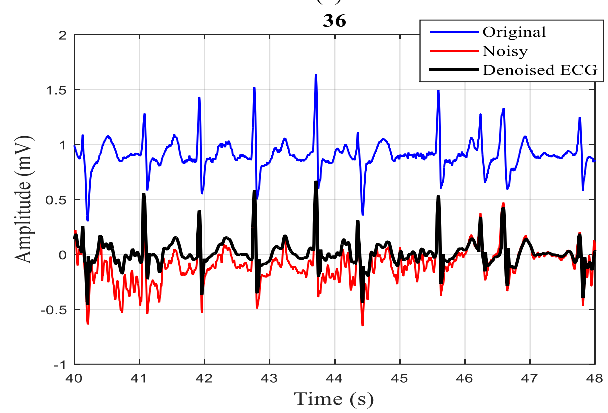

(b)

Fig.8- Performance of the proposed adaptive filter bank in the presence of MA noise for records a) 209 from ADB at SNR = 6dB b) 36 from SCDB at SNR= 8dB

It is worth noting that in our algorithm, the exact locations of R-peaks are not that important. Because our goal is not to detect and concatenate QRS complexes. Our goal is to identify high

This is the accepted manuscript (postprint) of the following article:
Hesar, H. D., & Mohebbi, M. (2020). An adaptive Kalman filter bank for ECG denoising. *IEEE journal of biomedical and health informatics*, *25*(1), 13-21.
https://doi.org/10.1109/JBHI.2020.2982935

frequency parts of ECG signals and chain them together for processing and do the same thing for the low-frequency parts. It does not matter whether the high frequency parts are real QRS complexes or not. What matters is that we separate the high frequency parts and low frequency parts and feed them to two independent adaptive Kalman filters. In other words, whether the Pan-Tompkins method, correctly or incorrectly identifies a location in an ECG signal as an R-peak, we know for sure that that location and its neighboring samples belong to a high frequency component. This knowledge is enough for us for separation of high and low-frequency components.

VI. Conclusion

To sum up, the adaptive Kalman filter bank proposed in this paper is able to solve a major drawback of model-based filtering that is handling signals with different kinds of morphologies without using a predefined model. This property is very beneficial in applications such as Holter monitoring in which ECG signals contain various kinds of beats and dynamics. Another challenge that we intended to resolve in this paper is use of simple and fast preprocessing steps instead of time-consuming heavy preprocessing steps. Our filter bank exhibited acceptable performance at low input SNRs in both stationary and non-stationary environments from both SNR improvement and MSEWPRD viewpoints. The proposed algorithm was compared with several popular ECG denoising methods such as wavelet transform, empirical mode decomposition and band pass filter. The comparison results showed that the proposed method outperformed EMD, WD and BPF in the presence of various ECG morphologies in both stationary and non-stationary environments at low input SNRs.

References

[1] O. Sayadi and M. Shamsollahi, "A model-based Bayesian framework for ECG beat segmentation," *Physiological Measurement,* vol. 30, no. 3, pp. 335-352, 2009.

[2] O. Sayadi and M. B. Shamsollahi, "ECG denoising and compression using a modified extended Kalman filter structure," *IEEE Trans. Biomedical Engineering,* vol. 55, no. 9, pp. 2240-2248, 2008.

[3] R. Sameni, M. B. Shamsollahi, C. Jutten, and G. D. Clifford, "A nonlinear Bayesian filtering framework for ECG denoising," *IEEE Trans. Biomedical Engineering,* vol. 54, no. 12, pp. 2172-2185, 2007.

[4] H. Hesar and M. Mohebbi, "ECG Denoising Using Marginalized Particle Extended Kalman Filter with an Automatic Particle Weighting Strategy," *IEEE Journal of Biomedical and Health Informatics,* vol. 21, no. 3, pp. 635-644, 2016.

[5] H. D. Hesar and M. Mohebbi, "An Adaptive Particle Weighting Strategy for ECG Denoising Using Marginalized Particle Extended Kalman Filter: an Evaluation in Arrhythmia Contexts," *IEEE Journal of Biomedical and Health Informatics,* vol. 21, no. 6, pp. 1581-1592, 2017.

[6] P. E. McSharry, G. D. Clifford, L. Tarassenko, and L. A. Smith, "A dynamical model for generating synthetic electrocardiogram signals," *IEEE Trans. Biomedical Engineering,* vol. 50, no. 3, pp. 289-294, 2003.

[7] A. Bryson Jr and L. Henrikson, "Estimation using sampled data containing sequentially correlated noise," *Journal of Spacecraft and Rockets,* vol. 5, no. 6, pp. 662-665, 1968.

[8] P. Zarchan, *Progress In Astronautics and Aeronautics: Fundamentals of Kalman Filtering: A Practical Approach* vol. 208: Aiaa, 2005.

[9] R. H. Shumway and D. S. Stoffer, "Time series analysis and its applications," *Studies In Informatics And Control,* vol. 9, no. 4, pp. 375-376, 2000.

[10] J. Hartikainen, A. Solin, and S. Särkkä, "Optimal filtering with Kalman filters and smoothers," *Department of Biomedica Engineering and Computational Sciences, Aalto University School of Science: Greater Helsinki, Finland,* vol. 16, 2011.

[11] S. Gibson and B. Ninness, "Robust maximum-likelihood estimation of multivariable dynamic systems," *Automatica,* vol. 41, no. 10, pp. 1667-1682, 2005.

[12] D. Simon, *Optimal state estimation: Kalman, H infinity, and nonlinear approaches*: John Wiley & Sons, 2006.

[13] Z. Ghahramani and G. E. Hinton, "Parameter estimation for linear dynamical systems," Technical Report CRG-TR-96-2, University of Totronto, Dept. of Computer Science1996.

[14] G. Chang, "On kalman filter for linear system with colored measurement noise," *Journal of Geodesy,* vol. 88, no. 12, pp. 1163-1170, 2014.

[15] S. Kurl, T. H. Mäkikallio, P. Rautaharju, V. Kiviniemi, and J. A. Laukkanen, "Duration of QRS complex in resting electrocardiogram is a predictor of sudden cardiac death in men," *Circulation,* vol. 125, no. 21, pp. 2588-2594, 2012.

[16] The MIT-BIH Normal Sinus Rhythm Database. PhysioNet, Cambridge, MA [Online]. Available: http://www.physionet.org/physiobank/database/nsrdb/

[17] The MIT-BIH Arrhythmia Database [Online]. Available: http://physionet.org/physiobank/database/mitdb/

[18] Creighton University Ventricular Tachyarrhythmia Database [Online]. Available: https://physionet.org/physiobank/database/cudb/

[19] Sudden Cardiac Death Holter Database [Online]. Available: https://physionet.org/physiobank/database/sddb/

[20] The MT-BIH Noise Stress Test Database. PhysioNet, Cambridge, MA [Online]. Available: https://www.physionet.org/physiobank/database/nstdb/

[21] M. S. Manikandan and S. Dandapat, "Multiscale entropy-based weighted distortion measure for ECG coding," *IEEE Signal Processing Letters,* vol. 15, pp. 829-832, 2008.

[22] M. Blanco-Velasco, B. Weng, and K. E. Barner, "ECG signal denoising and baseline wander correction based on the empirical mode decomposition," *Computers in biology and medicine,* vol. 38, no. 1, pp. 1-13, 2008.

[23] S. Lahmiri, "Comparative study of ECG signal denoising by wavelet thresholding in empirical and variational mode decomposition domains," *Healthcare technology letters,* vol. 1, no. 3, p. 104, 2014.